

Autonomous implicit models of pinched hystereses with application to memristors

Abstract. This paper analyzes systems with an autonomous dynamics equivalent to that of mem-inductors and mem-capacitors. The systems have oscillatory inductive and capacitive pinched self-crossing hystereses that follow the folded saddle dynamics around the origin and two equilibria of the center type, each located on the opposite sides of singularity (impasse curve). When parameters of the systems change to yield an increased frequency of oscillations, then the areas enclosed by the hystereses decrease. The time zero-crossing property of the systems is also discussed.

Streszczenie. W artykule dokonano analizy dynamiki pewnej klasy układów autonomicznych. Rozważane układy charakteryzują się indukcyjnymi i pojemnościowymi, ściśniętymi i przecinającymi się histerezami, powstającymi w dynamicznie siodła na falde wraz z dwoma punktami równowagi typu centrum, położonymi po przeciwnych stronach krzywej osobiwej z punktami impasowymi. Wraz ze zmianą parametrów prowadzącą do zwiększenia częstotliwości oscylacji obszar objęty histerezą zmniejsza się. Własność jednociennego zerowania się sygnałów w czasie jest również rozważana. (Autonomiczne uwiklane modele histerezowe z zastosowaniem do memristorów)

Keywords: memristive systems, hysteretic models, folded saddles, lemniscates

Słowa Kluczowe: układy memristorowe, modele histerezowe, siodła na falde, lemniskaty

Introduction

Each of the six basic mem-elements is typically described by the input-state-output model $y = g(x)u$, $x' = u$, where y , x and u stand for the output, state and input variables, respectively [1]-[3]. The output-input characteristics $y-u$ are of pinched self-crossing type with the y and u zero crossing occurring at the same time instants. Moreover, when the frequency of the input u increases, then the area enclosed by the pinched hysteresis decreases. Also, typically, for the frequency $f \rightarrow \infty$, the double-valued pinched hysteresis property diminishes and the $y-u$ characteristic tends to that of a single-valued one. Certain physical elements or phenomena may also have hystereses with decreasing area when f increases. The $y-u$ characteristics can also be of a tangential rather than self-crossing nature [4]. The input-state-output models are *non-autonomous* with u being a periodic forcing signal (for instance a sinusoidal one). It turns out, however, that the memristive nature and characteristics can also be found in oscillatory circuits with *autonomous* models. This paper shows two dual circuits as such examples. The most important feature of the circuits is the presence of a folded saddle in the circuits' two-dimensional phase portraits. However, such a saddle is not an equilibrium point, as it is a phase plane point placed on a singularity manifold. Trajectories can cross the singularity thanks to that folded saddle, a well-known property of implicit systems [5].

Circuits with folded saddles

Three parallel elements, inductor L , capacitor C and a nonlinear resistor with the voltage-current characteristic $v = \gamma + i^2$, $\gamma \in R$, can be analyzed through the equation

$$(1) \quad 2LC(x_1')^2 + 2LCx_1x_1'' + ax_1' = -\gamma - x_1$$

where x_1 is the current through the nonlinear resistor ($x_1 = i$) and $a = L$. A dual version of such a circuit with a series connection of the elements (nonlinear resistor has the current-voltage characteristic $i = \gamma + v^2$) is also described by (1) with x_1 being the voltage across resistor ($x_1 = v$) and $a = C$. Equivalently, we have implicit ODEs $A(\mathbf{x})\mathbf{x}' = B(\mathbf{x})$, $\mathbf{x} = (x_1, x_2)^T$ that describe both circuits, as follows

$$(2) \quad \begin{aligned} x_1x_1' &= \frac{1}{2b}x_2 \\ ax_1x_2' &= -\gamma x_1 - x_1^3 - \frac{a}{2b}x_2 \end{aligned}$$

where x_2 is the current through capacitor and $b = C$ in the parallel circuit, while x_2 is the voltage across inductor and

$b = L$ in the series circuit. To simplify discussion, let's assume that $L = 1 H$, $C = 1 F$. Then the nature of the point $(x_1, x_2) = (0, 0)$, which is located on the fold line $x_1 = 0$, depends on the value of γ . Notice that $A(0)$ is singular, and $b(0) = 0$. The origin is a folded saddle for $\gamma < 0$, folded saddle-node for $\gamma = 0$, folded node for $0 < \gamma < 1/8$, degenerate folded node for $\gamma = 1/8$, and a folded focus for $\gamma > 1/8$. There are trajectories crossing the fold line $x_1 = 0$ in the first four cases. No trajectory crossing $(0, 0)$ exists in the folded focus case.

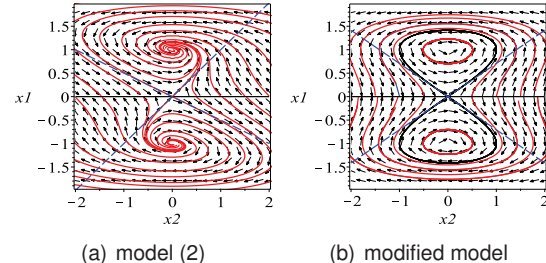


Fig. 1. Solutions of implicit autonomous models with parameters $a = b = 1$, $\gamma = -1$. Solutions cross the origin at the directions indicated by the dashed lines. Except for the origin, the fold curve $x_1 = 0$ consists of *impasse points* where trajectories terminate at or originate from. Two equilibria exist also at $(\pm 1, 0)$.

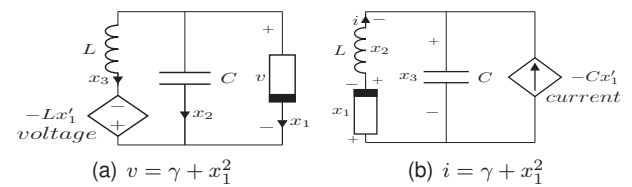
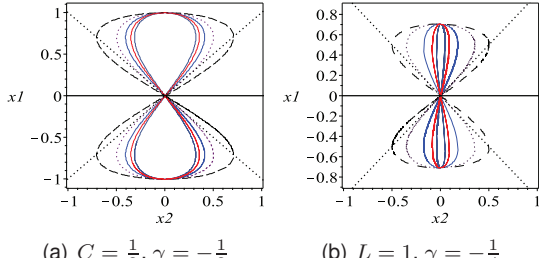


Fig. 2. Two dual mem-circuits described by the autonomous implicit model: $x_1x_1' = (1/2)b x_2$, $ax_2' = -\gamma - x_1^2$ (modified (2)).

Fig. 1(a) shows a phase portrait for $\gamma = -1$ with a folded saddle at the origin. Trajectory crosses the origin at $dx_1/dx_2 = \{-1/2, 1\}$. A stable and unstable equilibria exist at $(\sqrt{-\gamma}, 0)$ and $(-\sqrt{-\gamma}, 0)$, respectively, both with complex eigenvalues. Notice also that no periodic solution exists for any value of γ in the two circuits. The lack of periodic solution is changed if a modification of the circuit is introduced by adding the elements controlled by x_1' as shown in Figs. 2(a), 2(b). Such a modification yields a rather dramatic change in the dynamics of the circuits and, as shown in this paper, makes that the added elements have the characteristics of mem-elements. In particular, the added element in Fig. 2(a) has a pinched characteristic $\psi - x_3$ of a meminductor



(a) $C = \frac{1}{2}, \gamma = -\frac{1}{2}$ (b) $L = 1, \gamma = -\frac{1}{4}$

Fig. 3. Periodic solutions crossing the origin of the modified circuit in Fig.2(a): (a) $L = 1/4$ (dashed), $L = 1/2$, $L = 3/4$, $L = 1$, $L = 5/4$ (smallest loop), (b) $C = 4$ (dashed), $C = 2$, $C = 1/2$, $C = 1/8$, $C = 1/32$ (smallest loop).

(ψ =flux, x_3 =current), while the added element in Fig.2(b) has a pinched characteristic $q-x_3$ of a memcapacitor (q =charge, x_3 =voltage). The above modifications yield the model (1) without the ax'_1 term. This results in the second equation in (2) being modified to

$$(3) \quad ax'_2 = -\gamma - x_1^2$$

while the first equation in (2) does not change. There is also a change in the nature of the two equilibrium points ($\pm\sqrt{-\gamma}, 0$) in Fig.1(a), which now become centers with purely imaginary eigenvalues, as shown in Fig.1(b). The nature of the folded point $(0, 0)$ has not changed. The origin still remains a folded saddle with two trajectories crossing the fold $x_1 = 0$ from one side to the other. The above facts result in the pinched trajectories moving between the sides of $x_1 = 0$ and encircling the centers at $(\pm\sqrt{-\gamma}, 0)$. Thus the x_1 - x_2 trajectories are symmetrical as shown in Figs.3(a),3(b) for several values of L ($= a$) and C ($= b$). It can be shown for both circuits that the trajectories cross the origin at angles $dx_2/dx_1 = \pm\sqrt{-2b\gamma/a}$ ($\equiv \kappa$). Also, the period of oscillation of x_1 is $T = 2\pi\sqrt{ab}$ and, thus, the period of x_2 is $\pi\sqrt{ab}$, half the period of x_1 .

Theorem 1: The pinched trajectory (x_1, x_2) is such that the variables x_1 and $x_2\sqrt{-2b\gamma/a}$, $\gamma < 0$, satisfy the following equation

$$(4) \quad x_1^4 = c^2(x_1^2 - x_2^2)$$

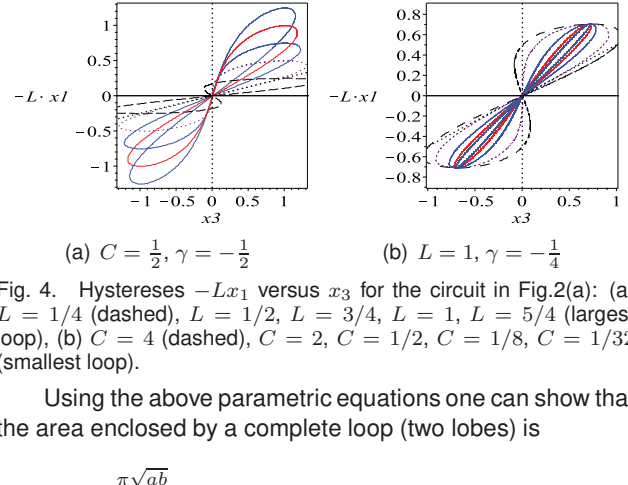
with $c^2 = -2\gamma > 0$.

Proof: The first equation in (2) and (3) yield $ax_2 dx_2 = -2(\gamma + x_1^2)bx_1 dx_1$, which, after integration takes the form $ax_2^2 = -2b\gamma x_1^2 - bx_1^4$. From the fact that the trajectory is pinched at $(0, 0)$ we obtain the constant of integration to be zero. Now, with the scaling $x_2 \rightarrow x_2\sqrt{-2b\gamma/a}$ (or equivalently $x_2^2 \rightarrow x_2^2(-2b\gamma/a)$) we obtain $ax_2^2(-2b\gamma/a) = -2b\gamma x_1^2 - bx_1^4$, which is equivalent to (4). \diamond

Since (4) is the lemniscate of Gerono [6] (see Appendix I), therefore the pinched hysteresis (x_1, x_2) of the two circuits is a scaled version of that lemniscate. In particular, the properties of the lemniscate of Gerono are modified by the factor of κ , which appears in the above theorem. This scaling factor applies to such properties of the lemniscate of Gerono as the area enclosed by the lemniscate, arc length, parameterized equations, polar formula and others. As shown above, variables x_1 and x_2 satisfy the following equation $ax_2^2 = -2b\gamma x_1^2 - bx_1^4$. One possible parametrization of such an equation is

$$(5) \quad x_1(t) = \sqrt{-2\gamma} \sin\left(\frac{t}{\sqrt{ab}}\right), \quad x_2(t) = -\gamma \sqrt{\frac{b}{a}} \sin\left(\frac{2t}{\sqrt{ab}}\right)$$

for $0 \leq t < 2\pi\sqrt{ab}$ (one complete loop of hysteresis).



(a) $C = \frac{1}{2}, \gamma = -\frac{1}{2}$ (b) $L = 1, \gamma = -\frac{1}{4}$

Fig. 4. Hystereses $-Lx_1$ versus x_3 for the circuit in Fig.2(a): (a) $L = 1/4$ (dashed), $L = 1/2$, $L = 3/4$, $L = 1$, $L = 5/4$ (largest loop), (b) $C = 4$ (dashed), $C = 2$, $C = 1/2$, $C = 1/8$, $C = 1/32$ (smallest loop).

Using the above parametric equations one can show that the area enclosed by a complete loop (two lobes) is

$$(6) \quad A = 2 \int_0^{\pi\sqrt{ab}} x_2 x'_1 dt \\ = -2\gamma \sqrt{\frac{-2\gamma}{a}} \int_0^{\pi\sqrt{ab}} \sin\left(\frac{2t}{\sqrt{ab}}\right) \cos\left(\frac{t}{\sqrt{ab}}\right) dt = -\kappa \frac{8\gamma}{3}.$$

Notice that the value of A in (6) is a scaled version of the corresponding value of the area of lemniscate of Gerono, $A_G = \frac{4}{3}c^2$ [6]. Thus we have $A_G = -\frac{8\gamma}{3}$ (since $c^2 = -2\gamma$ in (6)). This gives $A = \kappa A_G$.

One method of computing the arc length of the pinched hysteresis is to use parametric equations (5) to have

$$(7) \quad s = 4 \int_0^{\pi/(2\omega)} \sqrt{(x'_1)^2 + (x'_2)^2} dt \\ = 4 \int_0^{\pi/(2\omega)} \sqrt{\frac{2\gamma}{ab} \left(\frac{2\gamma b}{a} - 1 \right) - \frac{2\gamma}{ab} \left(\frac{8\gamma b}{a} - 1 \right) \sin^2(\omega t) + \frac{16\gamma^2}{a^2} \sin^4(\omega t)} dt$$

with $\omega = 1/\sqrt{ab}$. If we use the modified coordinates $(x_1, x_2\sqrt{-2b\gamma/a})$ with x_1 and x_2 as in (5), then the above formulas simplify as $ax_2^2 = -2b\gamma x_1^2 - bx_1^4$ becomes the lemniscate of Gerono. Notice the dependence of the areas of hystereses shown in Figs.3(a),3(b) on L and C , which determine frequency of oscillations f . This is discussed in more detail in the next section where an interesting interpretation of the $-ax_1$ - x_3 trajectory of the controlled elements is provided. With $x_3 = -x_1 - x_2$, the $-ax_1$ - x_3 characteristic has a typical interpretation of a mem-inductor and a mem-capacitor for the circuits in Figs.2(a) and 2(b), respectively.

Controlled elements as mem-inductors and mem-capacitors and their properties

The current through the controlled element and through L in Fig.2(a) is $x_3(t)$ and the controlled element's voltage is $V(t) = -Lx'_1(t)$. Thus, the integral of $V(t)$ is the flux $\psi(t) = \int V(t)dt = -Lx_1(t) + const$. Assuming, $const = 0$, the $-Lx_1(t)$ versus $x_3(t)$ graph is actually the flux-current characteristic of the controlled element. Similarly, in Fig.2(b) we have that the voltage across the controlled element and across C is $x_3(t)$ and the controlled element's current is $I(t) = -Cx'_1(t)$. Thus, we have $q(t) = \int I(t)dt = -Cx_1(t) + const$. Again, for $const = 0$, the $-Cx_1(t)$ versus $x_3(t)$ graph is actually the charge-voltage characteristic. Figs.4(a),4(b) show typical graphs of $-Lx_1$ versus x_3 obtained (for circuit in Fig.2(a)) by solving the first equation in (2) with (3) for several values of L , C and two values of γ . Figs.5(a),5(b) show the time responses of $x_3(t)$ and $-Lx_1(t)$ for two sets of parameters. Note that the areas of hystereses in Fig.4(a),4(b) can be computed with

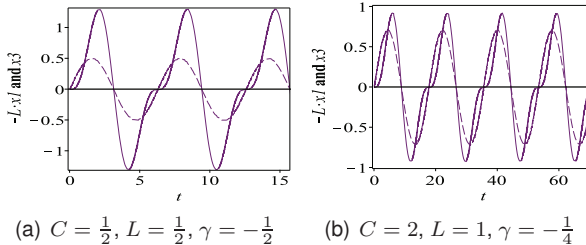


Fig. 5. Periodic solutions of $-Lx_1$ and x_3 for the dotted hystereses: (a) in Fig.4(a), (b) in Fig.4(b).

$x_3 = -x_1 - x_2$ as follows

$$(8) \quad \begin{aligned} A &= 2a \int_0^{\pi\sqrt{ab}} (-x_1 - x_2)(-x'_1) dt \\ &= 2a \int_0^{\pi\sqrt{ab}} (x_1 x'_1 + x_2 x'_1) dt \\ &= 2a(x_1^2/2) \Big|_0^{\pi\sqrt{ab}} + \int_0^{\pi\sqrt{ab}} x_2 x'_1 dt \\ &= -\frac{16a\gamma}{3} \sqrt{-2\gamma b} = \frac{-8\gamma\sqrt{-2\gamma}}{3\pi f} \end{aligned}$$

where we used the fact that $x_1^2/2 \Big|_0^{\pi\sqrt{ab}} = 0$ for $x_1(t)$ in (5) and $\int_0^{\pi\sqrt{ab}} x_2 x'_1 dt$ is computed in (6). Clearly, with increasing frequency f the areas of hystereses in Fig.4(a),4(b) decrease. This is a well-known fingerprint of most memristive elements. Also, the *identical zero time crossing property* of hysteresis $-ax_1-x_3$ is as follows. Transforming graphs from the (x_1, x_2) coordinate system into $(x_3, -ax_1)$ changes the line $x_1 = -x_2$ into $x_3 = 0$ (since $x_3 = -x_1 - x_2$), while the line $x_1 = x_2$ changes into $-ax_1 = ax_3/2$. Thus, the dotted lines in Figs.3(a),3(b), being the tangential lines for the loops with $L = \frac{1}{2}$, $C = \frac{1}{2}$ (Fig.3(a)) and $L = 1$, $C = 2$ (in Fig.3(b)), are changed to the dotted lines $-Lx_1 = \frac{1}{4}x_3$ in Fig.4(a) and $-Lx_1 = \frac{1}{2}x_3$ (in Fig.4(b)). The pinched hysteresis loops inside the sector determined by the dotted lines have the property that the zero crossings of $-Lx_1$ and x_3 occur at the same time instants. Hysteresis loops not entirely inside that sector, that is the dashed curves in Figs.4(a),4(b), do not have the zero crossing property. Those curves correspond to the dashed curves in Figs.3(a),3(b) intersecting the straight dotted lines $x_1 = \pm x_2$. The condition for the trajectories $-ax_1-x_3$ to have the zero crossing property for both mem-circuits is $\kappa \leq 1$.

Pinched hystereses due to Devil's curve

In this subsection, we discuss another modification of (2) yielding a hysteresis equivalent to Devil's curve [7]. Consider the following implicit equations

$$(9) \quad \begin{aligned} x_1 x'_1 &= \frac{1}{2ab}(ax_2 - 2bx_2^3) \\ ax'_2 &= -\gamma - x_1^2 \end{aligned}$$

Theorem 2: The oscillatory trajectory of (9), x_1 versus x_2 , is pinched at the origin for $\gamma < 0$ and $a/b > 0$, and satisfies the following equation

$$(10) \quad x_1^4 - x_2^4 = c^2 x_1^2 - d^2 x_2^2$$

with $c^2 = -2\gamma > 0$ and $d^2 = a/b > 0$.

Proof: From (9) we obtain $(ax_2 - 2bx_2^3)dx_2 = -2(\gamma + x_1^2)bx_1 dx_1$, which, after integration takes the form $ax_2^2 - bx_2^4 = -2b\gamma x_1^2 - bx_1^4$. From the fact that the trajectory is pinched at (0) we obtain the constant of integration to be zero. Simple rearrangement of terms and division by b in the last equation yield $x_1^4 - x_2^4 = -2\gamma x_1^2 - (a/b)x_2^2$. This is equivalent to (10). ◇

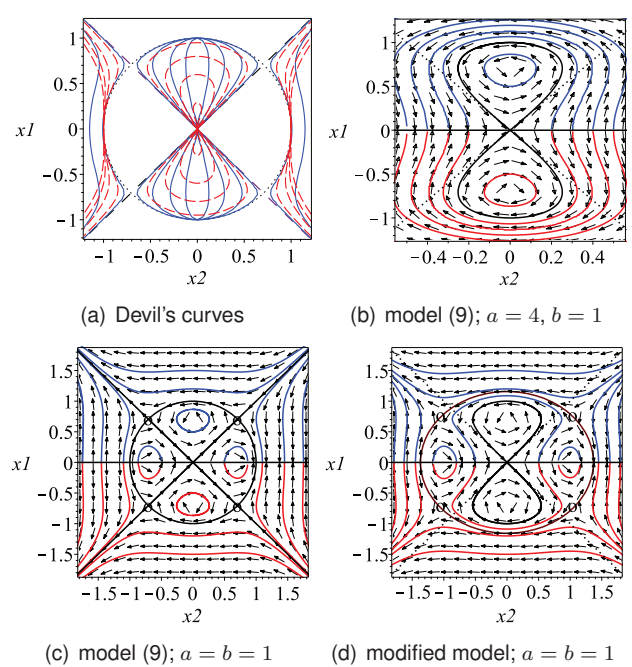


Fig. 6. (a) Devil's curves for various values of d^2 ($= a/b$) and $c^2 = 1$, see (10). (b) Pinched hysteresis passes through the origin as Devil's curve (10) with $c^2 = 1$ ($= -2\gamma$) and $d^2 = 4$ ($= a/b$). (c) Phase portrait with 4 saddles (marked by the \circ characters) away from the fold $x_1 = 0$, folded saddle and two folded centers at $x_1 = 0$. Two trajectories cross the fold line along the lines $x_1 = \pm x_2$. This is the degenerate Devil's lemniscate case (10) with $c^2 = d^2$, yielding $x_1^2 + x_2^2 = c^2$ in general, and with $c^2 = 1$ in the case illustrated in this plot. (d) Phase portrait of the modified system (with (11)) resulting in a pinched hysteresis through the origin. No other trajectories crossing the fold $x_1 = 0$ exist. The $\gamma = -1/2$ in all the cases above.

The graph of (10) is known as Devil's curve (or lemniscate) [7] and is shown for several parameters of a , b and γ in Fig.6(a) (in all cases the condition $c/d = \sqrt{-2\gamma b/a} > 1$ is satisfied). When the ratio c/d is less than 1, then the graphs in Fig.6(a) are rotated by 90 degrees. Each Devil's curve is of degree 4, has a crunode at the origin and the genus is equal 2. This does not allow for a birational parametrization. Other properties of the Devil's curve (area enclosed, parametrization, arc length, Abelian integrals, etc.) can be found in [7, 8]. Fig.6(b) shows a phase portrait with a hysteretic solution in the form of Devil's curve tangential to the lines $x_1 = \pm 2x_2$ at the origin. In the case $-2\gamma = a/b$ we obtain a degenerate Devil's curve - a circle. Such a case is shown in Fig.6(c). Two solutions along the straight lines $x_1 = \pm x_2$ pass through the folded saddle at the origin.

A modification, for example when the parameters a , b or γ bifurcate, is possible. This will yield a distorted Devil's curve equation, however, still yielding a pinched hysteresis at the origin. For example, by changing the first equation in (9) to

$$(11) \quad x_1 x'_1 = \frac{1}{2ab}(ax_2 - bx_2^3)$$

and keeping the second equation in (9) unchanged, we obtain the phase portrait as in Fig.6(d), where the four saddles (marked by \circ) do not result in a folded saddle at the origin anymore (as they do in Fig.6(c)). The folded saddle still remains intact (as in Fig.6(b)), allowing for a pinched hysteretic solution to travel through the origin in a periodic manner. No other periodic trajectory moving between different sides of the fold $x_1 = 0$ exists. It is a straightforward exercise to show that the hysteresis is described by (10) with the term x_2^4 replaced by $x_2^4/2$.

Further analysis of the hystereses in the form of Devil's curves and their transformations into the pinched, same time instant zero crossing memristive-like hystereses in the first and third quadrants are possible by defining a new variable, say x_3 ($= -x_1 - x_2$) in a way similar to that discussed earlier for the lemniscate of Gerono. Finally, it is worth pointing out that the pinched oscillatory hystereses considered in this paper are closely linked to planar conservative dynamical systems which are well researched and found many applications [9]. The following lemma links Devil's curve with the well-known Duffing's autonomous and undamped equation.

Lemma: The variable x_2 in (10), being a solution of (9) with the initial conditions $x_1(0)$ and $x_2(0)$, satisfies the following Duffing's equation $ax_2'' = -\frac{1}{b}x_2 + \frac{2}{a}x_2^3$, with the conditions $x_2(0)$ and $x_2'(0) = -(\gamma + x_1^2(0))/a$.

Proof: Duffing's equation for $x_2(t)$ can be easily obtained by differentiating the second equation in (9) and using the first equation to replace the term x_1x_1' obtained after differentiation. The initial condition $x_2'(0)$ follows from the second equation in (9) at $t = 0$. ◇

Parameters b and a control the linear stiffness and amount of non-linearity in the restoring force, respectively. The right-hand side in the above Duffing's equation, $-(1/b)x_2 + (2/a)x_2^3$, is the restoring force $F(x_2)$, provided by the non-linear spring, as we have $mx_2'' = F(x_2)$ with $m = a$.

Obtaining pinched hystereses numerically: a word of caution

All hystereses and time-series plots in this paper were created using *Maple 18*. Special care should be exercised in order to obtain hystereses. Some extra analysis of the directions at which a hysteresis crosses the origin is needed. Also, choosing the right numerical solver is important, as is a selection of that solver's optional parameters. For example, the *Gear* extrapolation method in *Maple 18* that was used in solving the *autonomous* ODEs in this paper, has two choices of the extrapolation procedure (Burlirsch-Stoer or polynomial extrapolation), each with about 18 optional parameters [10]. The Livermore stiff ODE solver *lode* has 8 choices for sub-methods, each with 16 optional parameters. The partial code in Appendix II illustrates how to successfully obtain both the pinched hysteresis in Fig.6(b) and the corresponding time-series solutions $x_1(t)$ and $x_2(t)$ by using the *Gear* method (with the default Burlirsch-Stoer rational extrapolation procedure) and only two optional parameters, *abserr* and *relerr*, specifying the desired accuracy of the solution.

Conclusion

The dynamics of the *autonomous*, *differentiable* and *implicit* models analyzed in this paper follow either the scaled lemniscate of Gerono (with the $\kappa = \sqrt{-2\gamma b/a}$ parameter) or Devil's curve. Both planar curves yield pinched, self-crossing hystereses resulting from a folded saddle located at a fold (singularity). The hystereses' areas of the controlled elements in the two dual *autonomous* circuits (associated with Gerono's lemniscate) decrease with an increased frequency.

Appendix II: Maple code

```
with(plots): with(DEtools): g:=-0.5: a:=4: b:=1:
eq1:=diff(x1(t),t)=(a·x2(t)-2·b·x2(t)^3)/(2·a·b·x1(t)): eq2:= a·diff(x2(t),t)=-g-x1(t)^2:
out:=dsolve({eq1,eq2,x1(0)=0.2e-5,x2(0)=0.1e-5},{x1(t),x2(t)},type=numeric,
method=gear,abserr=10^(-10),relerr=10^(-10)):
odeplot(out,[t,x1(t)], [t,x2(t)], -20..20, numpoints=5000)
odeplot(out,[x2(t),x1(t)], -20..20, numpoints=5000,color=black,axes=boxed,
thickness=2,view=[-0.55..0.55,-1.25..1.25],font=[label,"HELVETICA",20])
```

Analysis of the same time zero crossing property for the two circuits is also presented. The approach presented in this paper is based on *autonomous* models and it differs from the commonly used input-state-output *non-autonomous* model approach. Further extensions of the results in this paper to include autonomous dynamical models related to the lemniscates of Bernoulli and Booth seem also be possible.

Authors: Wiesław Marszałek, Rutgers University, Hill Center for Mathematical Sciences, 110 Frelinghuysen Road, Piscataway, NJ 00854, USA, email: w.marszalek@rutgers.edu. Research done at the Opole University of Technology in Poland. Financial support by the Fulbright Foundation in Washington, DC, USA is greatly appreciated.

REFERENCES

- [1] Marszałek W.: On the action parameter and one-period loops of oscillatory memristive circuits, Non. Dynamics, 82(1), pp. 619–628, 2015.
- [2] Marszałek W., Amdeberhan T.: Least action principle for mem-elements, J. Circuits, Systems and Computers, 24(10), 1550148, 2015.
- [3] Bielek Z., Bielek D., Biolkova V.: Hysteresis vs PSM of ideal memristors, memcapacitors, and meminductors, Electr. Lett., 52(20), pp. 1669–1671, 2016.
- [4] Marszałek W., Trzaska Z.: Dynamical models of electric arcs and memristors: the common properties, IEEE Trans. Plasma Science, 45(2), pp. 259–265, 2017.
- [5] Marszałek W., Amdeberhan T., Riaza R.: Singularity crossing phenomena in DAEs: a two-phase fluid flow application case study, J. Comp. Math. Appl., 49(2-3), pp. 303–319, 2005.
- [6] Weisstein E. W.: Eight curve. From Math World – A Wolfram Web Resource. [web page] <http://mathworld.wolfram.com/EightCurve.html>. [Accessed on 3 Oct. 2017.]
- [7] Weisstein E. W.: Devil's curve. From Math World – A Wolfram Web Resource. [web page] <http://mathworld.wolfram.com/DevilsCurve.html>. [Accessed on 3 Oct. 2017.]
- [8] Hilton H.: Plane Algebraic Curves, University Press (Oxford), 1920.
- [9] Hale J., and Koçak H.: Dynamics and Bifurcations, Springer-Verlag (Berlin), 1991.
- [10] Rovenski V., Walczak P.: Geometry and Its Applications, Springer-Verlag (Berlin), 2014.
- [11] Abbena E., Salamon S., Gray A.: Modern Differential Geometry of Curves and Surfaces with Mathematica, Chapman and Hall/CRC (Singapore), 2006.

Appendix I: Lemniscate of Gerono

Properties of the lemniscate of Gerono can be examined from the point of view of algebraic geometry in *Maple* by using its *algcurves* package [10]. The basic properties are [11]:

- Parameterization: $x_1 = c \frac{u^2 - 1}{u^2 + 1}$, $x_2 = c \frac{2u(u^2 - 1)}{(u^2 + 1)^2}$, $-\infty < u < \infty$. This parameterization results from the fact that the lemniscate of Gerono is of zero genus.
- Area of two lobes: $A_G = \frac{4}{3}c^2$
- Arc length:
$$\begin{aligned} s &= 4c \int_0^1 \sqrt{\frac{4x^4 - 5x^2 + 2}{1-x^2}} \\ &= 4c \int_0^{\pi/2} \sqrt{4\sin^4 t - 5\sin^2 t + 2} dt \\ &= 2\sqrt{2}c \int_0^{\pi/2} \sqrt{2 + \cos(2t) + \cos(4t)} dt \end{aligned}$$
- Polar equation: $r^2 = c^2 \sec^4 \theta \cos(2\theta)$
- Curvature: $k(t) = \frac{2\sqrt{2}\{2+\cos(2t)\}\sin t}{c\{2+\cos(2t)+\cos(4t)\}^{3/2}}$